IJPPR
INTERNATIONAL JOURNAL OF PHARMACY & PHARMACEUTICAL RESEARCH
An official Publication of Human Journals
ISSN 2349-7203
HUMAN

Human Journals
Research Article
July 2023 Vol.:27, Issue:4

Formulation and Evaluation Of In Vitro Characterization of Silymarin Loaded Proniosomes to Enhance the Oral Bioavailability

IJPPR
INTERNATIONAL JOURNAL OF PHARMACY & PHARMACEUTICAL RESEARCH
An official Publication of Human Journals
ISSN 2349-7203
HUMAN

Amit Chaudhary, Neha*,Chinu Kumari

Department of Pharmaceutics, Abhilashi College of Pharmacy, Abhilashi University, Chailchowk, Mandi, Himachal Pradesh , India.

Submitted: 30 June 2023
Accepted: 20 July 2023
Published: 30 July 2023

HUMAN JOURNALS
ijppr.humanjournals.com

Keywords: Silymarin, Proniosomes, Bioavailability, Investigation, Hepataobiliary.

ABSTRACT

Silymarin is a purified extract isolated from seeds of the milk thistle, Silybum marianum. Its main ingredients are the flavonolignans silybin, isosilybin, silydianine and silychristine. It is used to treat hepatobiliary illnesses. The aim of this investigation was to develop a procedure to improve the oral bioavailability of silymarin by using proniosomes. The preparation of silymarin loaded proniosomes done by slurry method. The response surface approach and design expert software were used to efficiently develop the optimal silymarin proniosomes based on the results of the screening process parameter. All the formulations were passed various evaluation parameters and they were found to be within limits.

INTRODUCTION :

Silymarin, which was purified from Silybum marianum L. Gaertn (milk thistle), is primarily composed of three flavonolignans, namely silybin, silydianin, and silychristin, the most active of which is silybin.. Silymarin, a well-known hepatoprotective, has been proven to be useful in treating a number of liver diseases, including alcoholic liver disease, acute and chronic viral hepatitis, hepatitis caused by toxins and drugs, and cirrhosis. Additionally, it was discovered to be successful in treating some cancers, including skin, prostate, and breast cancers. Silymarin works by inhibiting the binding of hepatotoxins to receptor sites on the membranes of hepatocytes, stabilising hepatocytes, and reducing glutathione oxidation to raise glutathione levels in the liver and intestines; antioxidant activity; stimulation of ribosomal RNA polymerase and subsequent protein synthesis, leading to enhanced hepatocyte regeneration.; antioxidant activity; stimulation of ribosomal RNA polymerase and subsequent protein synthesis, leading to enhanced hepatocyte regeneration. However, silymarin's limited water solubility and low bioavailability following oral administration have cast doubt on its efficacy as a treatment for liver illness. Silymarin taken orally is quickly absorbed, with a t max of 2-4 hours and a $t_{1/2}$ of 6 hours. Only 20 to 50 percent of oral silymarin, which is administered orally and goes through significant enterohepatic circulation, is ultimately absorbed from the gastrointestinal system. Only 3-8% are excreted in the urine, and 81% are eliminated in the bile as conjugates of glucuronide and sulphate. The concentration of silybin in the bile is 60 times more than that in the serum. Several strategies have been used to increase silymarin or silybin's bioavailability and rate of dissolution, including the formation of silybin-phosphatidylcholine complexes and the incorporation of solid dispersions.(1)

The dry and free-flowing proniosome powder was produced via a revolutionary production procedure to improve the chemical and physical stability of formulations and increase oral bioavailability of poorly water-soluble medicines. The process for making proniosome powder involves coating water-soluble carriers with surfactant and medication, specifically by covering each water-soluble carrier with dry surfactant and medication.(2)

MATERIALS AND METHODS:

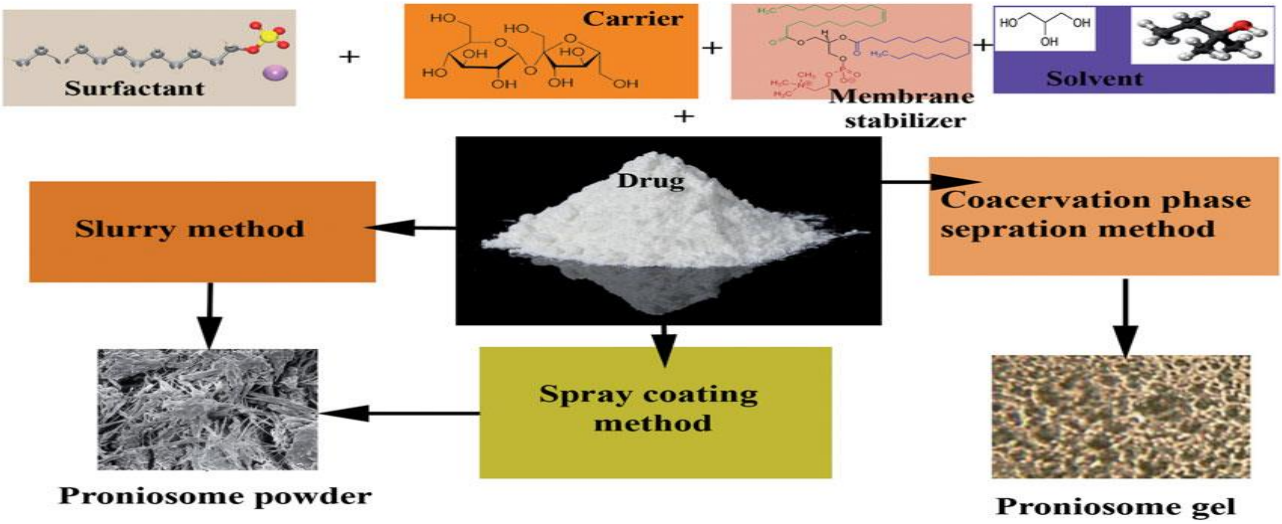

Figure 1.1. Illustration for materials and methods used for the preparation of proniosome.

Characterization of Proniosomes

Different parameters and techniques employed for characterization of proniosomes include measurement of vesicle size and size distribution, morphological characteristics, angle of repose, measurement of particle charge, rate of hydration (spontaneity), aerodynamic behavior, separation of unentrapped (free) drug, drug entrapment efficiency.

Measurement of angle of repose

Funnel method

The proniosomal powder was poured into the funnel, which was set in place, so that the funnel's exit orifice was 10 cm above the level of the surface. The angle of repose was further determined by measuring the cone's height and base diameter after the powder trickled down from the funnel to create one on the surface(3).

SEM

Proniosome particle size is a crucial consideration. Proniosomes' surface shape and size distribution were investigated using SEM. Aluminum stubs had double-sided tape attached to them, and the proniosomal powder was then applied to them. The scanning electron microscope's vacuum chamber contained the aluminium stub. The morphological characterization of the samples was observed using a gaseous secondary electron detector (3).

Measurement of vesicle size

The identical media that was utilized to create the vesicle dispersions was diluted approximately 100 times. On a particle size analyser, the size of the vesicles was assessed. The device consists of a small volume sample holding cell and a multi-element detector with a point focused at its center by a 632.8 nm He-Ne laser beam using a Fourier lens (R-5) with a minimum power of 5Mw. Before evaluating the vesicle size, the samples were agitated with a stirrer.(4)

Morphology of proniosomes

Proniosomal gels

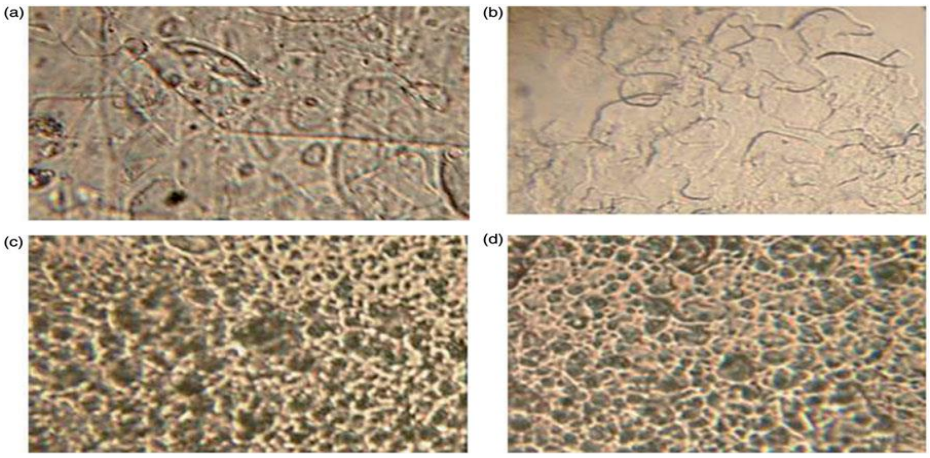

Figure 1.2: Photomicrograph of proniosomal gel of (a) Span 20/20% cholesterol, (b) Span 80/30% cholesterol, (c) Span 40/0% cholesterol and (d) Span 60/0% cholesterol (with permission from (4).

Proniosomal powders

Hu and Rhodes observed through the SEM that the surface of proniosome powder appeared to be smoother and have fewer fine features'' such as whiskers and sharp corners.(5)

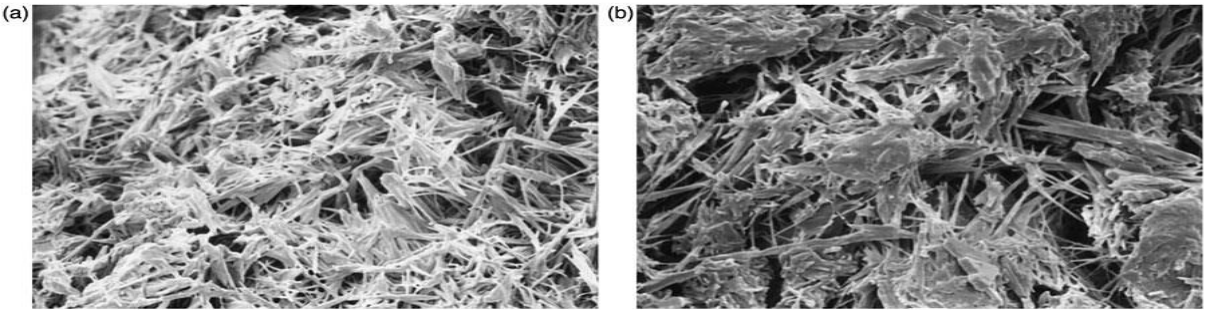

Figure 1.3: Photomicrograph of proniosomal powders (a) sorbitol carrier exhibits crystals with sharp edges and fine structure versus (b) proniosomal powder have somewhat less well-defined features (5)

Separation of unentrapped (free) drug

Dialysis

In dialysis techniques, the aqueous niosomal suspension is transferred to a dialysis tube suspended in a suitable dissolution media, the unentrapped drug is separated into the media through osmotic cellulose membrane at appropriate time intervals aliquots were withdrawn and analyzed for drug content by using suitable spectrophotometric and high-performance liquid chromatography (HPLC) methods(6).

Gel filtration

In gel filtration separation of unentrapped drug from niosomal dispersion is carried out by using a Sephadex-G-50column, eluted with suitable mobile phase and analyzed with suitable analytical techniques(7).

Centrifugation

Centrifugation is another technique used for separation of unentrapped drugs from niosomal suspension in which the pellets and supernatant are separated by centrifugation. The obtained pellets are washed and resuspended to get a niosomal suspension free from unentrapped drugs(8).

Entrapment efficiency

After separation of the unentrapped drug from the niosomal dispersions, the entrapment efficiency can be determined by complete disruption of the vesicles or by solubilizing the vesicles.(9)

Experimental Work

Table 1.1: List of Chemicals

S.NO.	Material	Source
1.	Silymarin	BioXpert Innovations Pvt. Ltd., India
2.	SPAN 60	Qualikems
3.	Cholesterol	Finar
4.	Methanol	Finar
5.	Disodium Hydrogen orthophosphate	Qualikems
6.	Potassium dihydrogen orthophosphate	Qualikems
7.	Sodium Hydroxide	Qualikems

Table 1.2: Lists of Instruments Used

S.No.	Equipment	Manufacturer
1.	Bath Sonicator	Raj Analytical Services,
2.	Electronic weighing balance	Sartorius
3.	Speed Regulator	Remi Equipment, Mumbai
4.	Magnetic stirrer	Contech Instruments Limited
5.	Cooling centrifuge	Systronic india, New delhi
7.	Dissolution Apparatus	Electrolab, Mumbai, India
8.	pH meter	Electrolab., Mumbai, India
9.	UV spectrophotometer	Electrolab Mumbai, India

2. Result and Discussion

2.1Preformulation studies

2.1.1Organoleptic properties: Organoleptic properties of silymarin was shown in Table 2.1.

Table 2.1: Observation of Organoleptic properties of silymarin

S.No.	Test	Specification	Observation
1.	Colour	**Yellow Brown Powder**	**Yellow Brown Powder**
2.	Odour	Slight and specific odour	Slight and specific odour
3.	Appearance	Bitter in taste	Bitter in taste

2.1.2 Melting point

The capillary method was used to determine silymarin's melting point. The information in Table 2.2 was nearly identical to the reference value, which attests to the drug's purity.

Table 2.2: Melting point of Silymarin

Drug	Specification	Observation
Silymarin	158°C	158.33^0C±0.58-160^0C±1.00

2.1.3. Determination of λ_{max} and calibration curve of Silymarin in methanol

2.1.3.1 Determination of λ_{max} of silymarin

Silymarin (10µg/ml) concentration showed maximum absorbance at 288 nm during scanning between 200 and 400 nm, which is consistent with published data as illustrated in Figure 2.1.

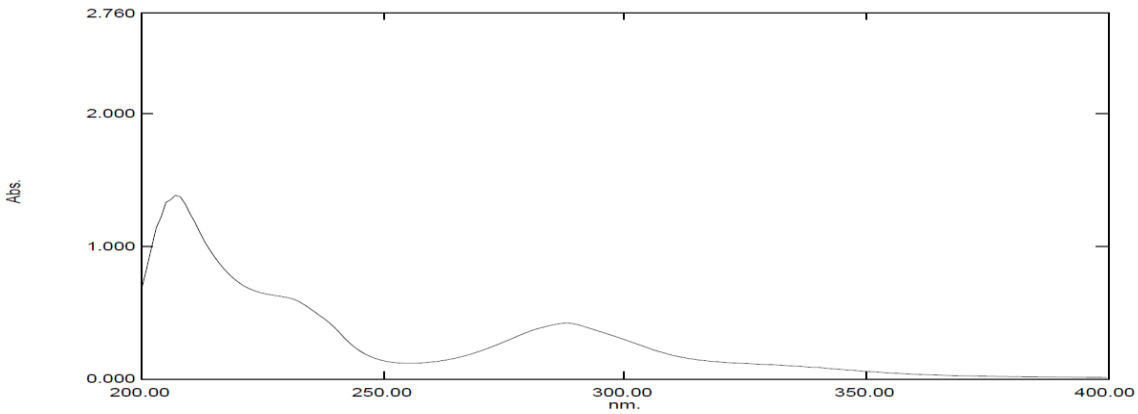

Figure 2.1: Graph of Absorption Maxima (λ_{max}) of silymarin in Methanol

2.1.3.2 Standard Calibration Curve of Silymarin in Methanol

A standard calibration curve was developed in the 2-20µg/ml range. The absorbance of silymarin solutions at various concentrations, as displayed in Table 2.3. The regression equation for Silymarin's calibration curve, which is depicted in figure 2.2, had an R^2 value of 0.999 and indicated good linearity with the value of Y = 0.0404x + 0.0062.

Table 2.3: Calibration curve between absorbance and concentration of Silymarin in methanol

Concentration (µg/ml)	Absorbance	STD
2	0.086	0.001
4	0.167	0.003
6	0.250	0.003
8	0.330	0.002
10	0.411	0.002
12	0.489	0.003
14	0.563	0.002
16	0.668	0.004
18	0.729	0.002
20	0.812	0.002

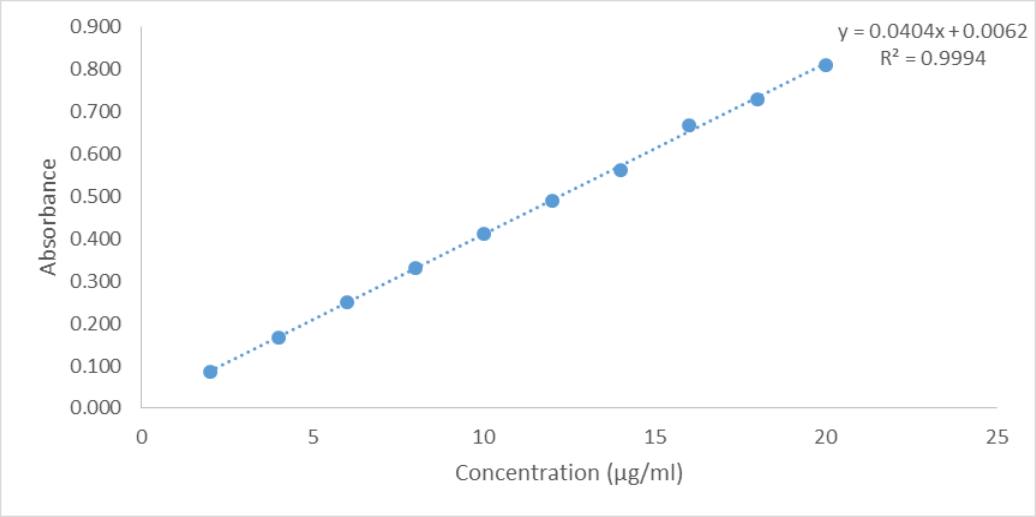

Figure 2.2: Graph of Standard Calibration Curve between absorbance and concentration of Silymarin in methanol

2.1.4 Solubility studies of drug

The drug's solubility in water, alcohols, chloroform, and phosphate buffer 6.8pH was assessed.

Table 2.4: Value of solubility (mg/ml) of silymarin in different solvents

S.No	Solvent	Solubility (mg/ml)
1	Water	0.495±0.007
2	Methanol	2.200±0.003
3	Ethanol	0.143±0.002
4	Chloroform	7.206±0.051
5	Phosphate Buffer 6.8pH	0.057±0.001

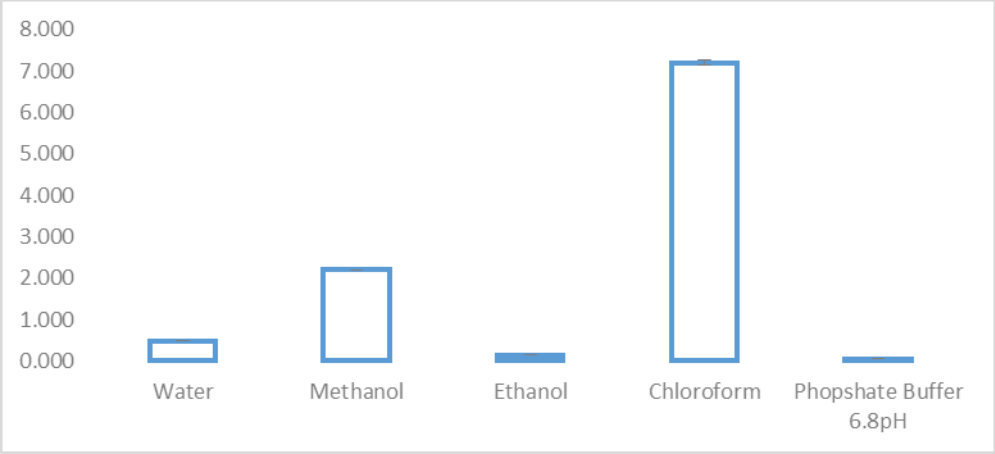

Figure 2.3: Bar Graph Solubility data of Silymarin in the different solvent medium

Silymarin demonstrated maximum solubility in chloroform, followed by methanol, and minimal solubility in pure water, as shown in Figure 2.3.

2.1.5 Partition coefficient of drug

Table 2.5 displays the partition coefficient of silymarin in the n-octanol: water mixture. Drugs having partition coefficients less than one are indicative of hydrophilic drugs, while those with log P greater than one are lipophilic in nature.

Table 2.5: Value of Partition coefficient of silymarin

S. No.	Drug	Reference partition coefficient	Observed Partition coefficient (Log P)	Nature of the drug
1.	Silymarin	1.41	1.467±0.016	Lipophilic (97)

2.2 Preparation of Silymarin loaded proniosmes

The slurry approach was successfully used to prepare Silymarin's pro vesicular systems. Due to the higher solubility of the drug and lipids in the combination of chloroform and methanol, this system was chosen as the solvent. Span 60 was employed in our work to help with stable vesicle production and to enhance the oral distribution of silymarin from proniosomes due to the high phase transition temperature (52°C). However, because cholesterol has a modulatory influence on the membrane bilayers, it can be introduced to the lipid phase to increase the

stability of the vesicles even though cholesterol alone does not form bilayers. Cholesterol was added because it can improve how hydrophilic medicines are encapsulated. (10)

2.3Screening of the process parameters

2.3.1 Effect of amount of the cholesterol

The effects of cholesterol concentrations ranging from 200µM to 800µM on proniosome production and silymarin drug entrapment % were studied.

Table 2.6: In vitro characterization parameters including percentage yield, percentage drug entrapment, percentage drug loading and micrometric properties

S.No.	Formulation code	Percentage yield (%)	Percentage drug entrapment (%)	Percentage drug loading (%)	Carr's index (%)	Hausner ratio
1	**SPN1**	92.90±0.303	75.47±0.13	15.67±0.03	2.142±1.709	1.022±0.018
2	**SPN2**	94.60±0.214	80.56±0.15	14.82±0.04	1.817±1.381	1.019±0.014
3	**SPN3**	97.40±0.207	97.94±0.12	15.99±0.02	5.140±1.027	1.054±0.011
4	**SPN4**	97.21±0.459	96.44±0.20	14.50±0.03	3.094±2.465	1.032±0.026

Table 7.6 showed that all prepared formulations increased in percentage of drug and drug loading of silymarin when various amounts of cholesterol were included. The efficiency of trapping has grown along with the content of cholesterol (SPN1 to SPN3). This might be adequately explained by the fact that the inclusion of cholesterol increases the bilayer's hydrophobicity and stability while also reducing its permeability, allowing for the effective intercalation of hydrophobic drugs with increased drug payload within the bilayer's hydrophobic core.

2.3.2 Effect of amount of span 60

The development of proniosomes and the proportion of drug entrapment of silymarin into the proniosomes were studied in a range of 200µM to 800µM of span 60.

Table 2.7: In vitro characterization parameters including percentage yield, percentage drug entrapment, percentage drug loading and micrometric properties

S.No.	Formulation code	Percentage yield (%)	Percentage drug entrapment (%)	Percentage drug loading (%)	Carr's index (%)	Hausner ratio
1	**SPN5**	97.17±0.099	79.17±0.17	16.11±0.03	2.650±0.566	1.027±0.006
2	**SPN6**	98.49±0.406	89.75±0.16	16.06±0.04	2.066±1.977	1.021±0.021
3	**SPN7**	98.80±0.329	98.27±0.19	15.82±0.03	6.955±0.469	1.075±0.005
4	**SPN8**	94.93±0.238	96.21±0.22	14.34±0.02	7.044±1.456	1.077±0.039

Table 2.7 showed that all prepared formulations increased in percentage drug loading and drug loading of silymarin when various amounts of the span 60 were present.

The percentage drug loading, percentage drug entrapment and percentage drug loading the silymarin drug was found to be in a range of the 94.93±0.430% to 98.80±0.329%, 79.17±0.17% to 98.27±0.19%, 14.34±0.02% to 16.11±0.03%. Furthermore, the micrometric properties including Carrs index and Hausner ratio of all prepared formulations were found to be in a range of the 2.650±0.566% to 7.044±1.456%, 1.021±0.006 to 1.077±0.039. Among all formulations, formulation SPN7 has the highest drug entrapment and drug loading.

2.4 Optimization of silymarin-loaded proniosomes

The response surface approach and design expert software were used to efficiently develop the optimal silymarin proniosome based on the results of the initial screening of the process parameters. The design space was established using the formulation parameters' effective operating ranges, such as the ranges for cholesterol and span 60 (400µM to 600µM). The main design was chosen expressly to maximize the input variables, and its components were described in Tables 2.8 and 2.9.

Table 2.8: Summary of the central composite design

Factor	Name	Units	Low Actual	High Actual	Low Coded	High Coded	Mean
X1	Amount of SPAN 60	micromolar	400	600	-1.00	1.00	500
X2	Amount of cholesterol	micromolar	400	600	-1.00	1.00	500
Y1	Percentage drug entrapment						

Table 2.9: Composition of the formulations prepared in central composite design with response

Formulation code	Factor 1 X1: Amount of SPAN 60 (micromolar)	Factor 2 X2: Amount of cholesterol (micromolar)	Response 1 Percentage drug entrapment (%)
DSPN1	641.421	500	99.61
DSPN 2	400	400	78.88
DSPN 3	500	358.578	81.68
DSPN 4	500	500	97.84
DSPN 5	500	641.421	88.69
DSPN 6	358.578	500	78.68
DSPN 7	500	500	98.85
DSPN 8	500	500	98.71
DSPN 9	400	600	80.17
DSPN 10	500	500	98.53
DSPN 11	600	600	98.17
DSPN 12	600	400	90.78
DSPN 13	500	500	97.91

A central composite design with two independent variables at five distinct levels was used to evaluate the effect on the dependent variables. As s, a total of 13 formulations were produced in accordance with the experimental strategy and further described for responses% drug entrapment. The data gathered from experimental runs was subjected to regression analysis.

The polynomial model equation shows how the linear, interaction, and quadratic model elements (represented by input variables X1, X2, and X1X2) influence the percentage of drug entrapment.

Percentage drug entrapment = $98.368+7.4374X1+2.324X2+1.525X1X2-4.652X1^2-6.6327X2^2$

According to the positive sign for the coefficient of X1, X2, and X1X2, as the percentage of entrapment rises, so does the concentration of components X1 and X2, as well as the combined influence of the two factors up to a certain concentration.

Table 2.10: ANOVA analysis

Source	Sum of Squares	df	Mean Square	F Value	p-value Prob > F	
Model	902.6078	5	180.5215652	1128.208564	< 0.0001	significant
X1-Amount of SPAN 60	442.5237	1	442.5236617	2765.64733	< 0.0001	
X2-Amount of cholesterol	43.21542	1	43.21541745	270.0840976	< 0.0001	
X1X2	9.3025	1	9.3025	58.13798563	0.0001	
$X1^2$	150.5954	1	150.595357	941.178253	< 0.0001	
$X2^2$	306.0409	1	306.0408526	1912.668497	< 0.0001	
Residual	1.120051	7	0.160007264			
Lack of Fit	0.255971	3	0.085323615	0.394980166	0.7643	not significant
Pure Error	0.86408	4	0.21602			
Cor Total	903.7279	12				
Std. Dev.	0.400009		R-Squared	0.998760633		
Mean	91.42308		Adj R-Squared	0.99787537		
C.V. %	0.437536		Pred R-Squared	0.996491906		
PRESS	3.170362		Adeq Precision	77.40953353		

By associating increases in the concentration of the span 60 and cholesterol with increases in the percentage of drug entrapment, the Figure 2.1 response surface plot further outlined the relationship between the dependent and independent variables.

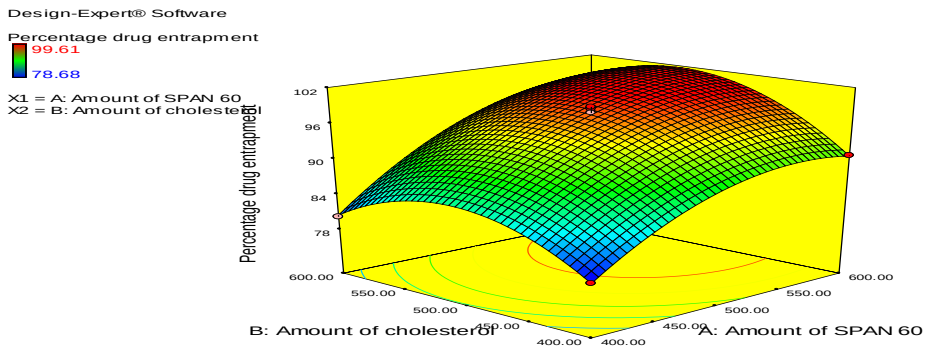

Figure 2.4: 3D response graph

Figure 2.4 showed that more space would become available in the proniosomes for the accommodation of the silymarin as the concentration of the span 60 increased. Up to a particular concentration, the hydrophobic interaction between hydrophobic drugs also boosts the percentage of silymarin drug entrapment. However, when the concentration of the span 60 was increased further, no further improvement of the drug entrapment and drug loading was shown.

The efficiency of entrapment has grown along with the content of cholesterol.

Table 2.11: Composition of the optimized formulation

Formulation code	Amount of SPAN 60 (µM)	Amount of cholesterol (µM)	Percentage of drug entrapment (%)	Actual Percentage drug entrapment (%)
DSPN 14	591.32	588.54	99.371	99.583±0.071

2.5 Evaluation of Silymarin loaded Proniosomes

2.5.1 Percentage yield

Table 2.12: Percentage yield of all prepared formulations

Formulation code	Percentage yield (%)
DSPN1	99.467±0.311
DSPN2	99.087±0.338
DSPN3	99.704±0.246
DSPN4	99.181±0.190
DSPN5	99.553±0.258
DSPN6	99.582±0.282
DSPN7	99.725±0.133
DSPN8	99.619±0.254
DSPN9	99.766±0.251
DSPN10	99.699±0.308
DSPN11	99.535±0.314
DSPN12	99.822±0.259
DSPN13	99.522±0.207
DSPN14	99.141±0.366

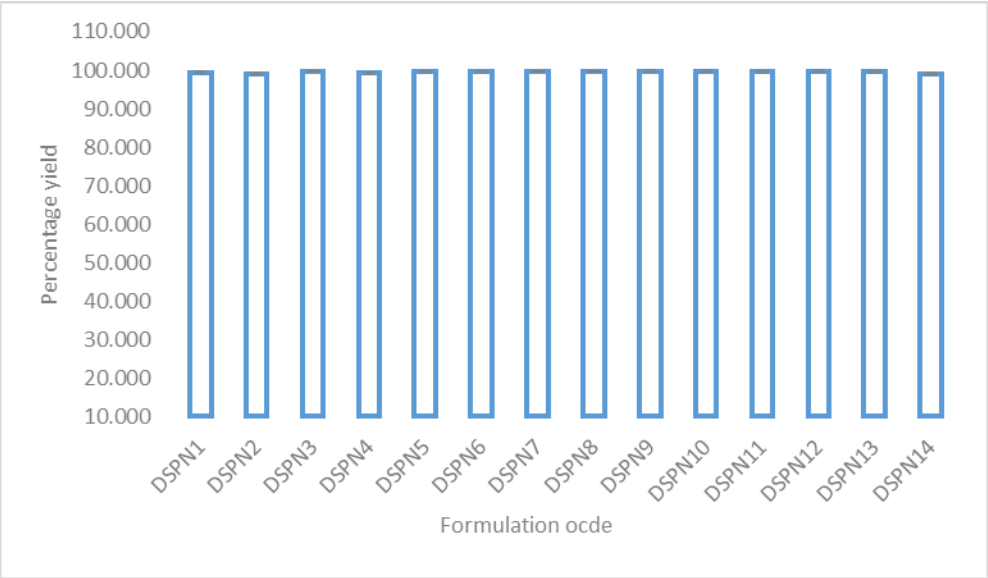

Figure 2.5: Bar graph of Percentage yield of all prepared formulations

The range of the percentage yield for all prepared formulations was shown in Table 2.12 to be between 99.087±0.338% to 99.821±0.259%.

2.5.2 Percentage drug entrapment and percentage drug loading

Table 2.13: Percentage of drug entrapment of all prepared formulations

Formulation code	% Drug entrapment (%)
DSPN1	99.606±0.102
DSPN2	78.885±0.147
DSPN3	81.678±0.082
DSPN4	97.838±0.201
DSPN5	88.692±0.127
DSPN6	78.685±0.197
DSPN7	98.852±0.114
DSPN8	98.711±0.074
DSPN9	80.170±0.154
DSPN10	98.534±0.216
DSPN11	98.168±0.267
DSPN12	90.778±0.127
DSPN13	97.909±0.124
DSPN14	99.580±0.070

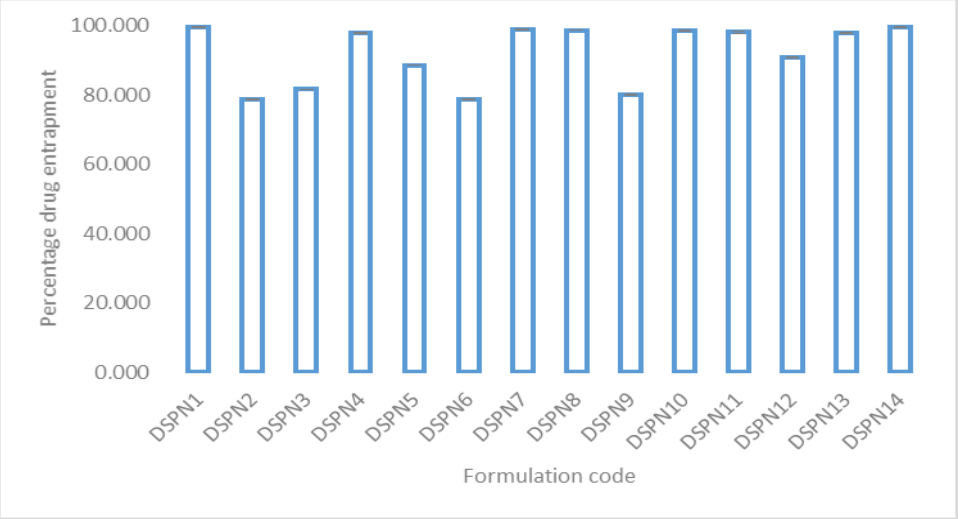

Figure 2.6: Graph of percentage drug entrapment of all prepared formulations

Table 2.14: Value and states of percentage drug loading of all prepared formulations

Formulation code	Percentage drug loading (%)
DSPN1	16.311±0.017
DSPN2	15.547±0.029
DSPN3	15.416±0.015
DSPN4	17.293±0.036
DSPN5	14.617±0.021
DSPN6	14.995±0.038
DSPN7	17.376±0.020
DSPN8	17.370±0.013
DSPN9	14.165±0.027
DSPN10	17.325±0.038
DSPN11	15.684±0.043
DSPN12	15.854±0.022
DSPN13	17.246±0.022
DSPN14	15.991±0.011

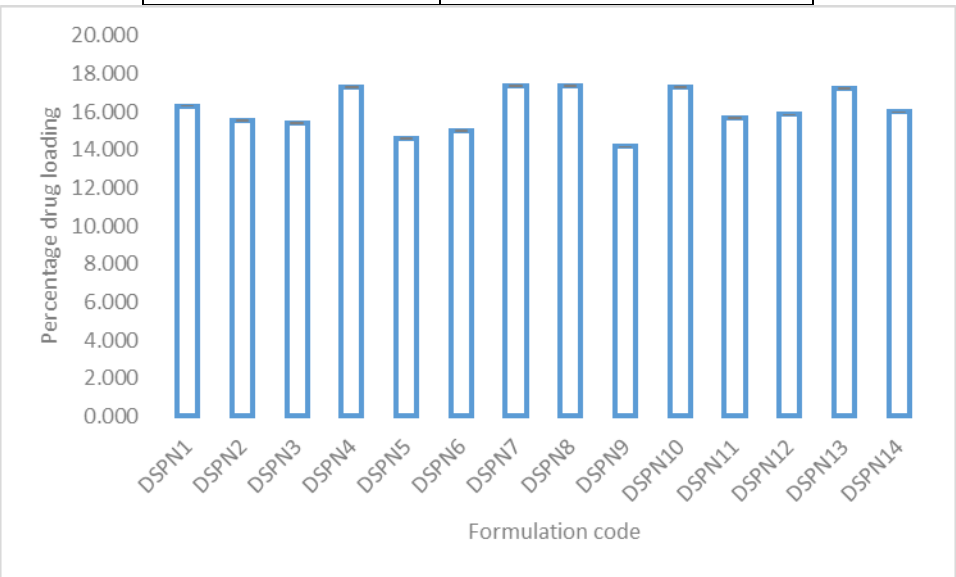

Figure 2.7: Graph of percentage drug loading of all prepared formulations

The percentage drug entrapment and percentage drug loading of all prepared formulations were determined to be in the ranges of 78.685±0.197% to 99.606±0.102%, 14.165±0.027% to 17.376±0.020%, respectively, according to Tables 2.13 and 2.14. The improved formulation's

percent drug loading and percent drug entrapment were found to be respectively 99.580±0.070% and 15.991±0.011%.

2.5.3Micromeritic properties of prepared formulation

Micromeritic properties of all prepared formulations were shown in Table 2.15.

Table 2.15: Micromeritic properties of all prepared formulations

Formulation Code	Bulk density (gm/cm^3)	Tapped density (gm/cm^3)	Carrs index (%)	Hausner ratio
DSPN1	0.158±0.001	0.161±0.002	2.164±1.601	1.022±0.017
DSPN2	0.157±0.001	0.160±0.002	1.567±1.631	1.016±0.015
DSPN3	0.158±0.002	0.165±0.001	5.300±1.029	1.056±0.011
DSPN4	0.156±0.002	0.164±0.001	4.932±1.489	1.052±0.016
DSPN5	0.161±0.001	0.167±0.002	3.821±0.920	1.040±0.010
DSPN6	0.159±0.003	0.162±0.003	1.776±1.987	1.018±0.021
DSPN7	0.154±0.004	0.165±0.001	6.877±0.771	1.074±0.009
DSPN8	0.151±0.002	0.163±0.004	7.324±1.432	1.079±0.017
DSPN9	0.153±0.002	0.164±0.001	6.931±0.564	1.075±0.006
DSPN10	0.154±0.001	0.161±0.002	4.321±1.090	1.045±0.012
DSPN11	0.161±0.003	0.162±0.003	1.006±0.079	1.010±0.001
DSPN12	0.159±0.002	0.163±0.004	1.996±0.822	1.020±0.009
DSPN13	0.156±0.003	0.158±0.001	1.539±0.673	1.016±0.007
DSPN14	0.151±0.001	0.157±0.001	2.224±0.796	1.034±0.001

For all prepared formulations, it was discovered that the bulk density, tapped density, carr's index, and hausner ratio all fell within the following ranges: 0.151±0.001gm/cm^3 to 0.161±0.001001gm/cm^3, 0.157±0.001001gm/cm^3 to 0.167±0.002001 gm/cm^3, 1.006±0.079% to 7.324±1.432%, 1.016±0.007 to 1.079±0.017. Tapped density, carr's index, bulk density, and Hausner ratio data for the optimized formulation was found to be 0.151±0.001001 gm/cm^3, 0.157±0.001001 gm/cm^3, 2.224±0.796% and 1.034±0.001.

On the basis of above evaluation parameters, DSPN14 formulation was selected for further evaluation.

2.5.4 Particle size and Zeta Potential

Table 2.16: Vesicle size, PDI and Zeta Potential of DSPN14 formulation

S.No.	Formulation code	Vesicle size (nm)	PDI	Zeta Potential (mv)
1	DSPN14	348.9	0.122	-21.8

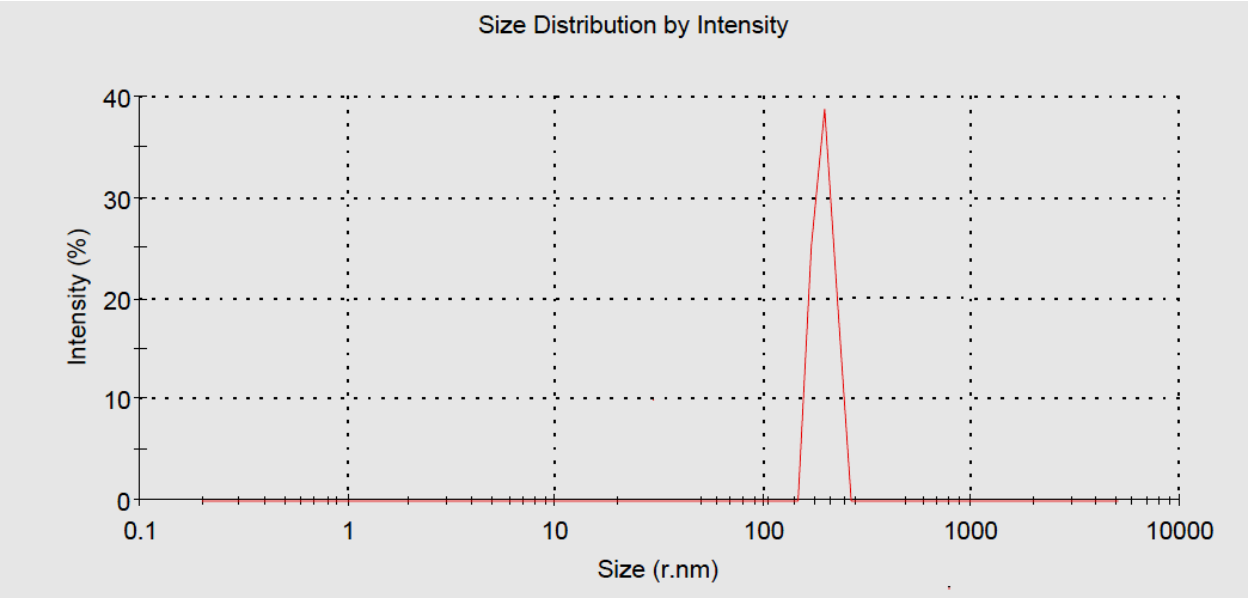

Figure 2.8: Globule size distribution graph of DSPN14 formulation

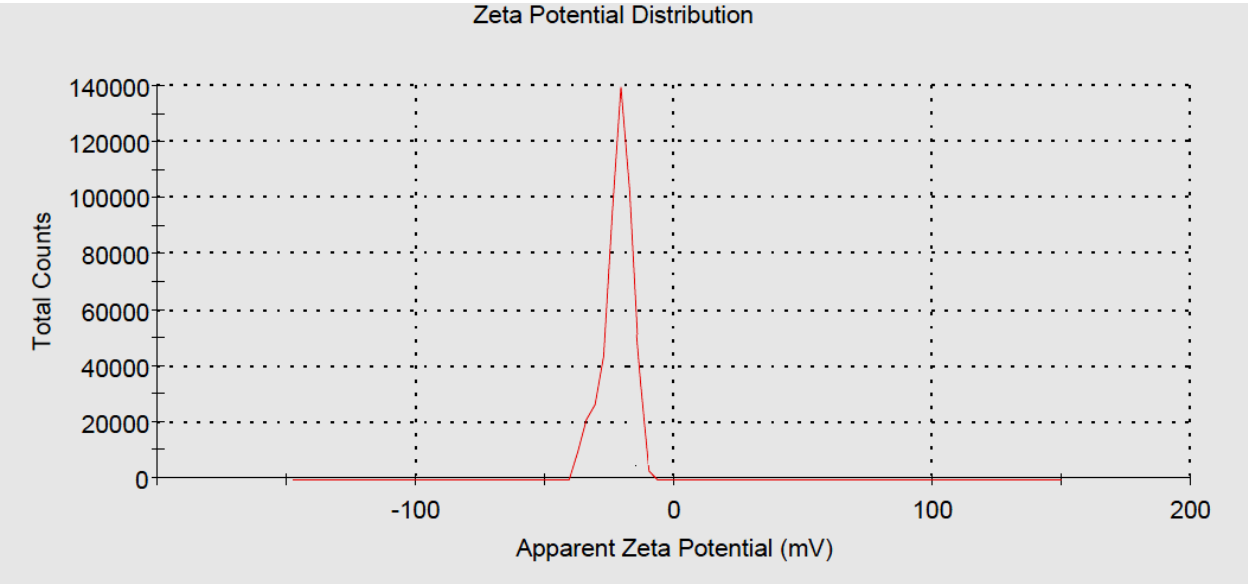

Figure 2.9: Zeta Potential distribution graph of DSPN14 formulation

It was discovered that the optimized formulation DSPN14's globule size and PDI value were 348.9 nm and 0.122. (Figure 2.8). In addition to the negative zeta potential that is implied by the arrangement of these emulsifiers at the oil-water interface and the various polar head groups that make up lecithin, they also impart a negative (21.8 mV) (Figure 2.9).

2.5.5 Identification of pure drug (FT-IR spectra)

FTIR spectrum of pure drug silymarin and the optimized formulation was shown in figure 2.10-2.11

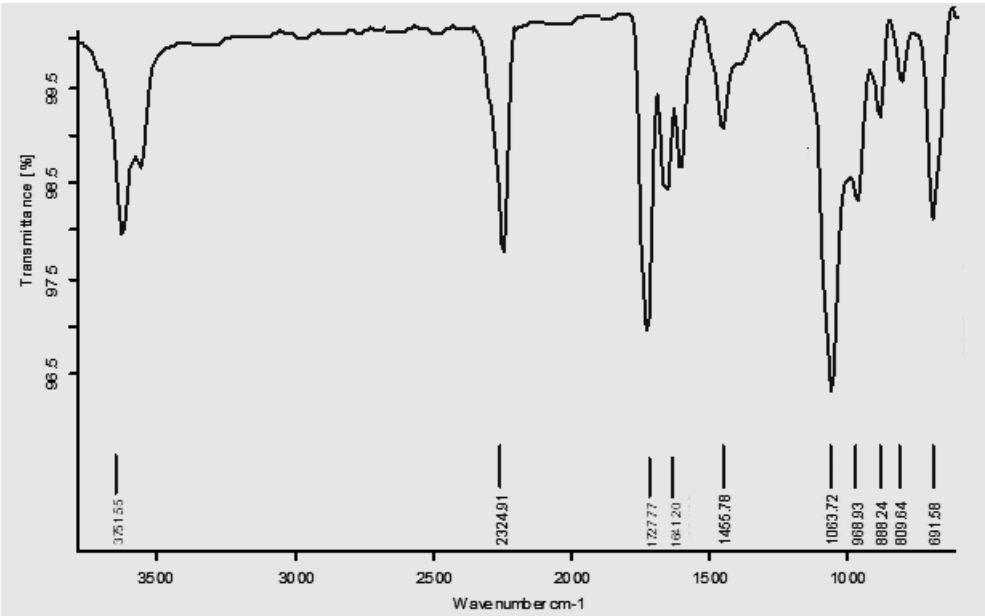

Figure 2.10: Graph of FTIR spectrum of silymarin

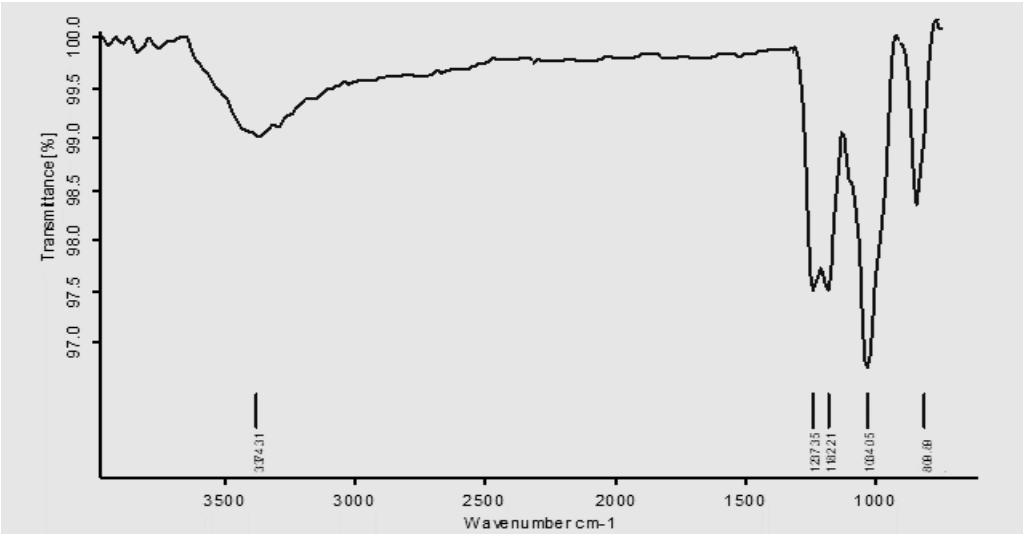

Figure 2.11: Graph of FT-IR Spectra of Silymarin loaded proniosomes

Transmission electron microscopy

TEM micrograph indicated a homogeneous distribution of small, spherical globules of the nisomes. (Figure 2.12)

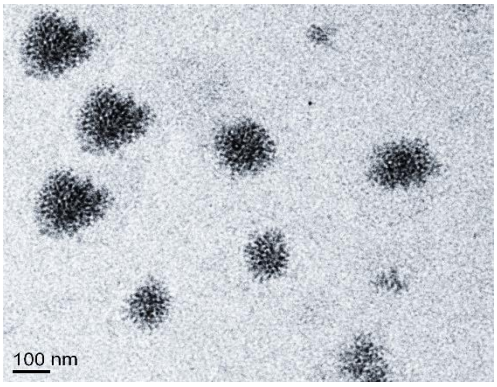

Figure 2.12: TEM micrograph of formulation DSPN14

2.5.7 Percentage dissolution of the silymarin-loaded proniosomes formulation

Comparison of the percentage dissolution between pure drug and silymarin loaded proniosomes shown in Table 2.17.

Table 2.17 : Value and states of Percentage drug study of percentage dissolution between pure drug and silymarin loaded proniosomes

Time (min.)	% Dissolution of pure drug in 0.1HcL	% Dissolution of pure drug in Phosphate buffer pH 6.8	% Dissolution of formulation DSPN14 in 0.1HcL	% Dissolution of formulation DSPN14 in Phosphate buffer pH 6.8
0	0.00±0.00	0.00±0.00	0.00±0.0	0.00±0.00
5	3.840±0.056	3.163±0.113	65.228±0.338	84.701±0.340
10	7.237±0.068	8.955±0.203	93.135±0.563	94.965±0.675
20	10.156±0.070	11.024±0.023	95.044±0.565	97.113±0.338
30	14.238±0.090	14.103±0.034	98.624±0.225	97.670±0.228
60	14.326±0.056	14.652±0.045	98.181±0.113	98.704±0.338
120	14.533±0.011	14.708±0.035	99.341±0.118	98.943±0.225

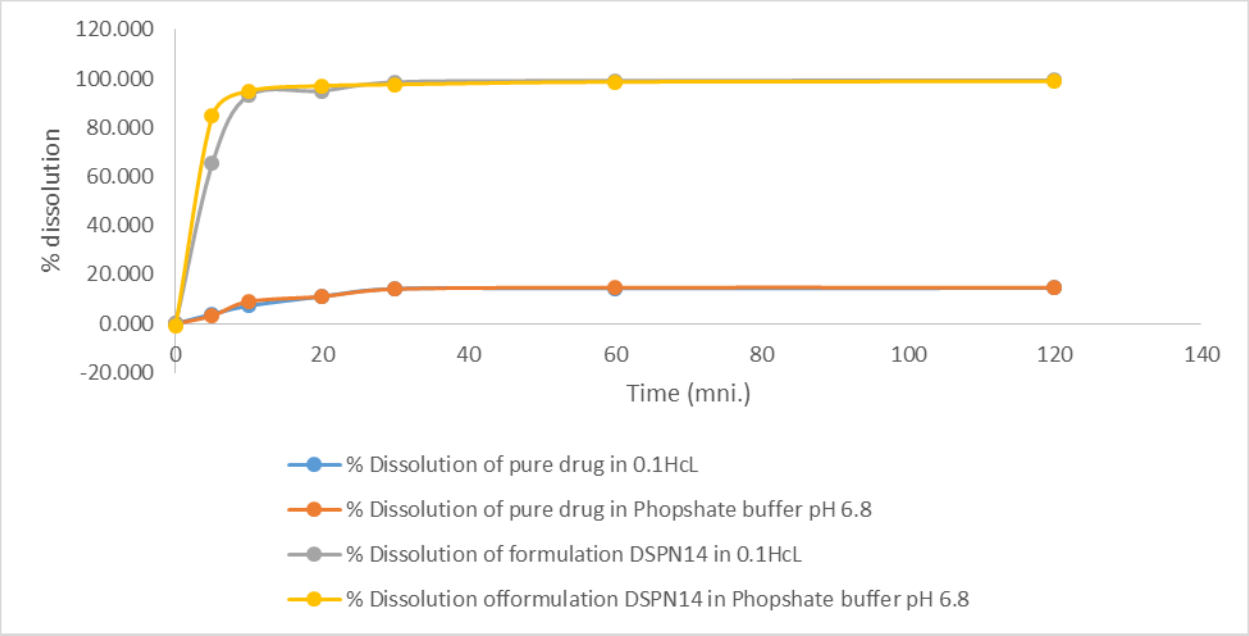

Figure 2.13: Comparison of the in-vitro dissolution profile of the pure drug and silymarin-loaded proniosome powder in different media

According to Table 2, after 30 minutes, the amount of silymarin that was dissolving from the proniosome was more than 97-98% in both buffer HCl (pH 1.2) and phosphate buffer solution (pH 6.8), as opposed to the 14-15% of pure silymarin drug from the pure drug. Because silymarin is more soluble in proniosomes, this might be the case. This was most likely brought about by the fact that silymarin was dispersed in the proniosome powder in a molecular or amorphous state, and that the proniosome powder's vast surface area increased the drug's rate of drug dissolution, resulting in faster dissolution.

2.5.8 In vitro drug release study

Figure 2.14 and Table 2.18 illustrated silymarin releases from proniosome formulations and pure drug suspension.

Table 2.18: Comparison of the in vitro drug release profile of the silymarin from a pure drug suspension and proniosome powder

Time (hr.)	% Drug release of pure drug suspension	% Drug release of formulation DSPN14
0	0.00±0.0	0.00±0.0
0.25	7.367±0.22	16.597±0.113
0.5	15.562±0.46	22.961±0.338
1	19.699±0.25	29.406±0.450
2	23.121±0.20	39.908±0.455
4	27.815±0.24	53.672±0.563
8	31.952±0.23	68.630±0.570
10	37.442±0.20	82.155±0.250
12	37.999±0.16	97.749±0.788
24	38.396±0.18	99.261±0.450

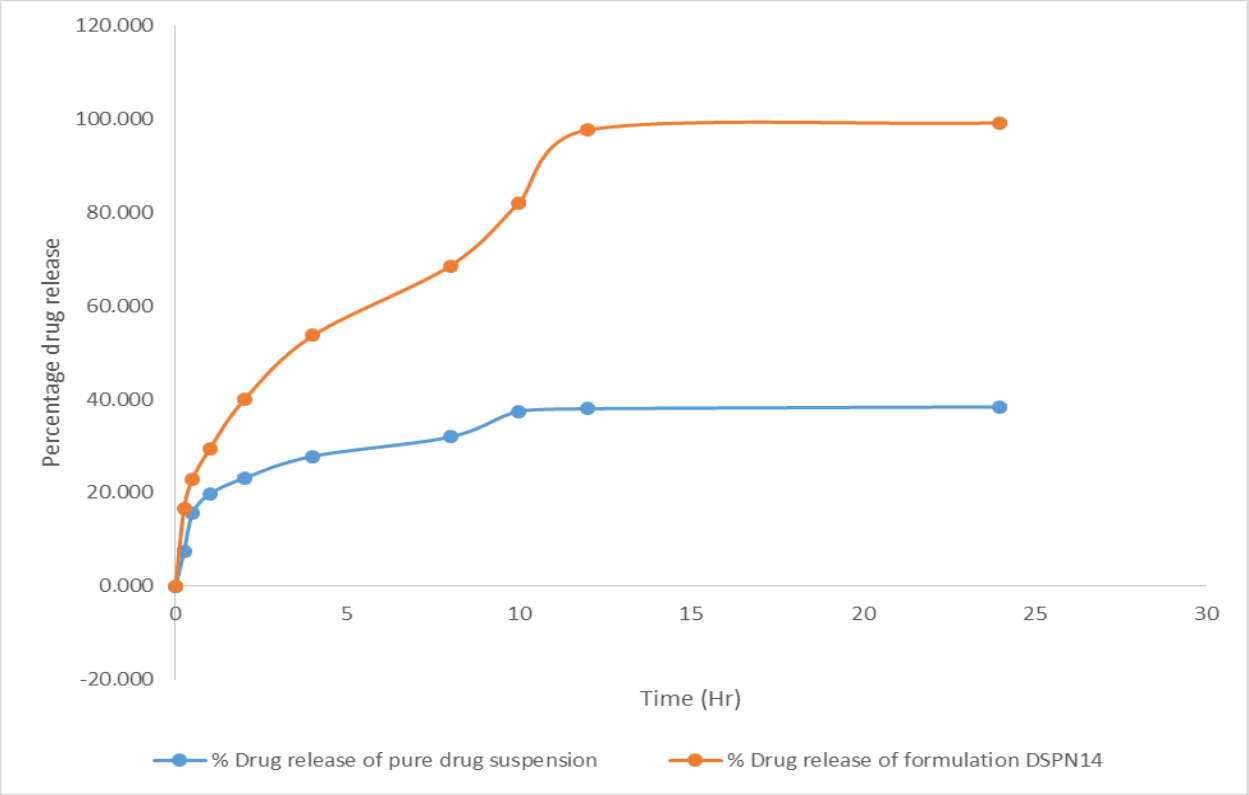

Figure 2.14: Comparison of the in vitro drug release profile of the silymarin from pure drug suspension and proniosome powder DSPN14

In buffer solution (pH 1.2 or 6.8), proniosome formulation released silymarin at a rate that was significantly higher than that of the pure drug suspension. In comparison to proniosome formulation, silymarin pure drug suspension released 38.396±0.18% of the medication after 24 hours while proniosome formulation released 99.261±0.450%.

2.5.9 Percentage drug release kinetic study

Percentage drug release kinetics parameters of the release of the silymarin from the optimized proniosome formulations DSPN14

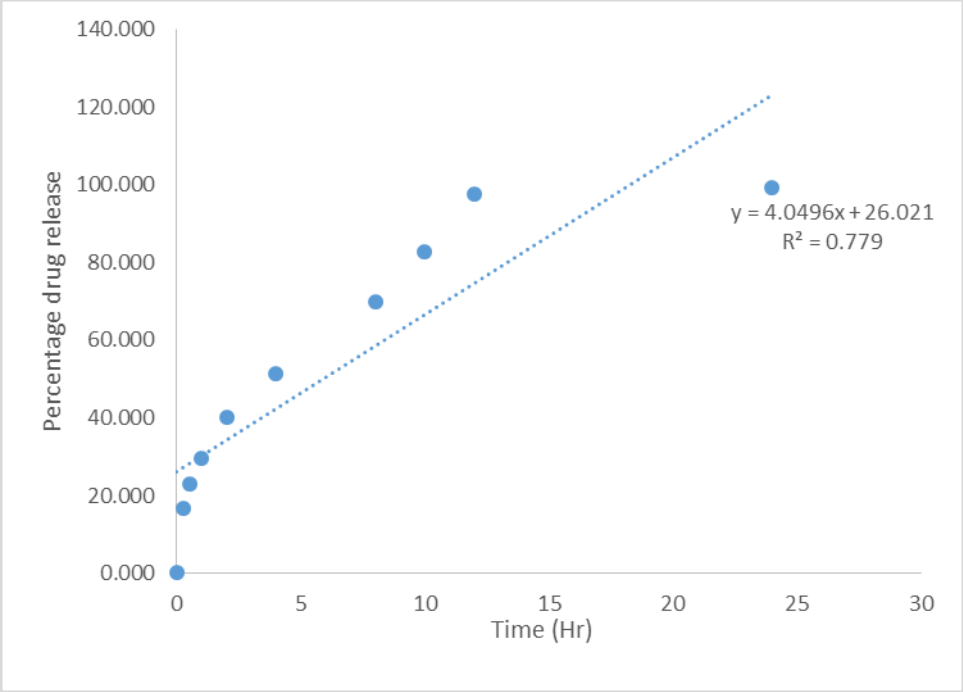

Figure 2.15: Zero order kinetic model

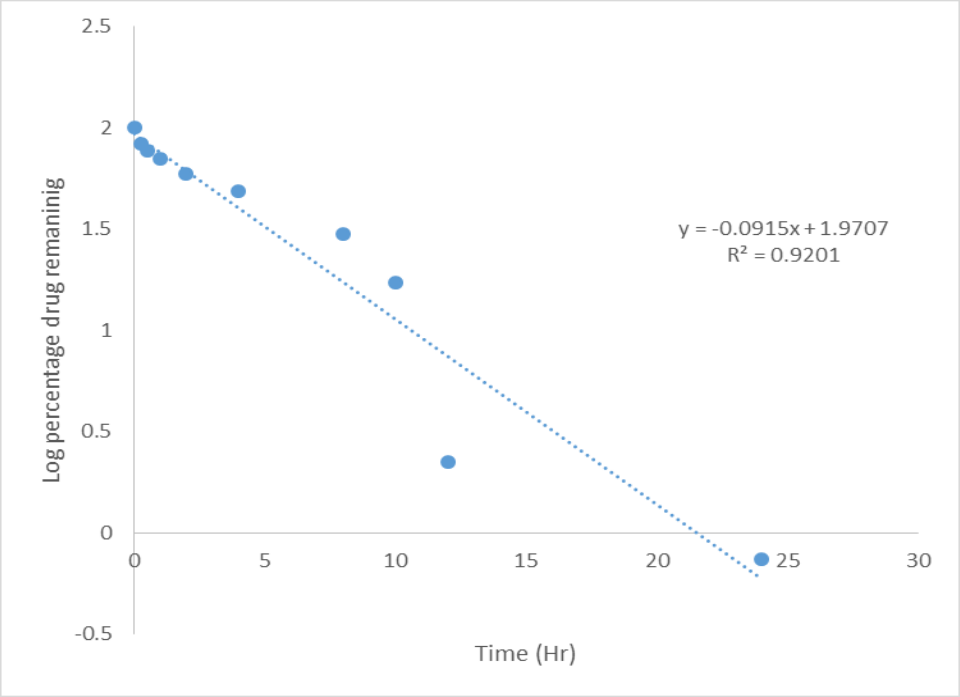

Figure 2.16: First order kinetic model

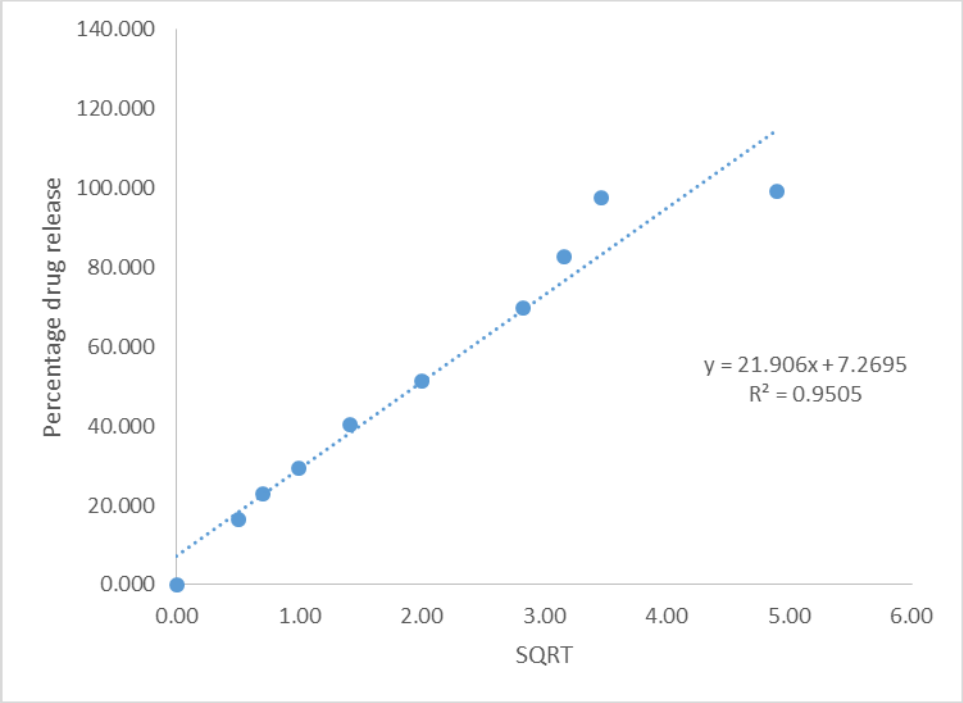

Figure 2.17: Higuchi order kinetic model

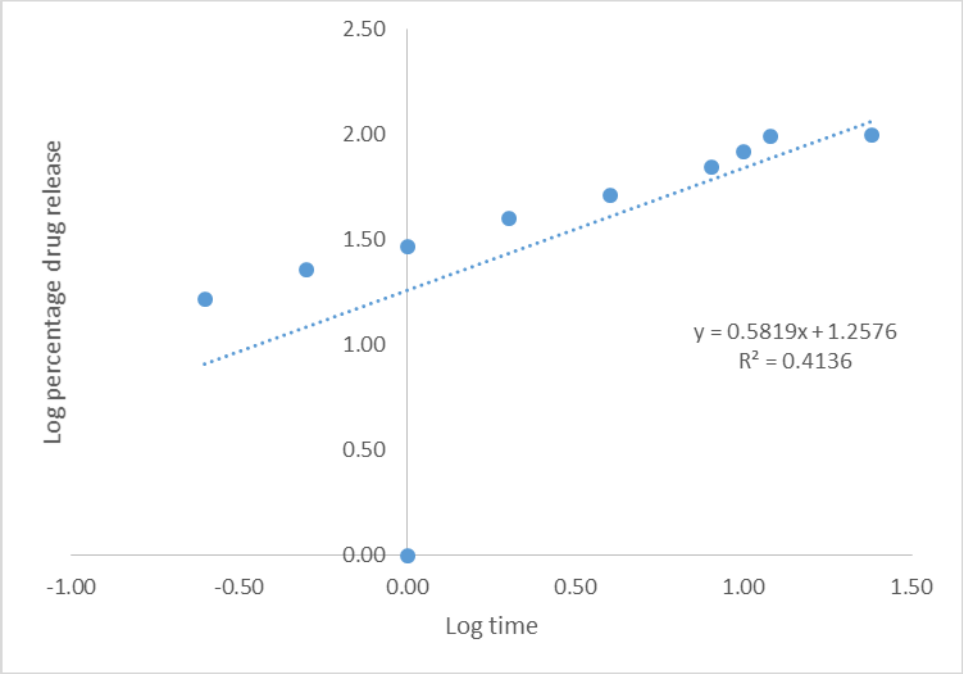

Figure 2.18: Korsmeyer Peppas order kinetic model

The Higuchi model, which has a greater value of the regression coefficient than the other models, best explains the release of silymarin from the proniosome formulations, according to Figures 2.15-2.18.showed the highest absorbance at 288nm when.

CONCLUSION:

The silymarin loaded proniosome was produced for the current investigation to enhance silymarin's oral bioavailability and dissolution. The melting point of silymarin was found to be 158.330C±0.58-1600C±1.00 during preformulation research. Silymarin (10µg/mll) concentration showed highest absorbance at 288nm when scanned between 200 and 400nm. By drawing a graph between the absorbance and concentration, a standard calibration curve was constructed in the range of 2-20µg/ml. With an R2 value of 0.999, the regression equation Y = 0.0404x + 0.0062 demonstrated good linearity. Silymarin had the highest solubility in chloroform, followed by methanol, and had the lowest solubility in pure water. Silymarin's n-octanol:water partition coefficient reveals that the medication has a lipophilic character. Using a previously described slurry approach, proniosome of Silymarin were effectively produced.In preliminary screening research, cholesterol levels and span 60 molecules from 200µM to 800µM were examined in relation to proniosome production and the proportion of silymarin that was entrapped in proniosomes. The optimal silymarin proniosome was swiftly prepared using the response surface approach and design expert software based on the results of the initial screening of the process parameters. The design space was established using the effective operating ranges of the formulation parameters, such as the amounts of cholesterol (400–600µM) and span 60 (400–600µM). A three-dimensional graph showed that as the concentration of the span 60 increased, more space in the proniosomes became available for silymarin encapsulation. Up to a particular concentration, the hydrophobic interaction between hydrophobic drugs also boosts the percentage of silymarin drug entrapment. However, when the concentration of the span 60 was increased further, no further improvement of the drug entrapment and drug loading was shown. The efficiency of entrapment has grown along with the content of cholesterol. This might be adequately explained by the fact that the inclusion of cholesterol increases the hydrophobicity and stability of the bilayer while also reducing its permeability. This effectively intercalates hydrophobic drugs into the bilayer's hydrophobic core, resulting in an increased drug payload. The results with high cholesterol content, however, could not be extrapolated, and on the contrary, the entrapment values decreased as the cholesterol concentration in the formulation increased. Higher levels of cholesterol may compete with the drug for packing space in the bilayer during the development and may also disrupt the bilayer's linear regular structure, which would impede the accommodation of drug molecules. The final optimized formulation was prepared with a composition of the Amount of SPAN 60

and Amount of cholesterol is 591.32µM and 588.54µM. The range of the percentage yield for all prepared formulations was found to be between 99.087±0.338% to 99.821±0.259%. The percentage drug entrapment and percentage drug loading of all prepared formulations were determined to be in the ranges of 78.685±0.197% to 99.606±0.102%, 14.165±0.027% to 17.376±0.020%, respectively. The improved formulation's percent drug loading and percent drug entrapment were found to be respectively 99.580±0.070% and 15.991±0.011%. The finding of the study suggested the optimized formulation DSPN14's globule size and PDI value were 348.9 nm and 0.122.. In addition to the negative zeta potential that is implied by the arrangement of these emulsifiers at the oil-water interface and the various polar head groups that make up lecithin, they also impart a negative (21.8 mV). TEM micrograph indicated a homogeneous distribution of small, spherical globules of the nisomes. After 30 minutes, the amount of silymarin that was dissolving from the proniosome was more than 97-98% in both buffer HCl (pH 1.2) and phosphate buffer solution (pH 6.8), as opposed to the 14-15% of pure silymarin drug from the pure drug. Because silymarin is more soluble in proniosomes, this might be the case. This was most likely brought about by the fact that silymarin was dispersed in the proniosome powder in a molecular or amorphous state and that the proniosome powder's vast surface area increased the drug's rate of drug dissolution, resulting in faster dissolution. In vitro drug release study, In buffer solution (pH 1.2 or 6.8), proniosome formulation released silymarin at a rate that was significantly higher than that of the pure drug suspension. In comparison to proniosome formulation, silymarin pure drug suspension released 38.396±0.18% of the medication after 24 hours while proniosome formulation released 99.261±0.450%.The Higuchi model, which has a greater value of the regression coefficient than the other models, best explains the release of silymarin from the proniosome formulations.

CONFLICT OF INTEREST

The authors have no conflicts of interest regarding this investigation**.**

ACKNOWLEDGMENTS

The authors would like to thank their parents, all the members of the Department of Pharmaceutics Abhilashi College of Pharmacy, Chailchowk , Mandi HP for their constant support and guidance.

REFERENCES

1) Wu W, Wang Y, Que L. Enhanced bioavailability of silymarin by self-microemulsifying drug delivery system. European Journal of Pharmaceutics and Biopharmaceutics. 2006;63(3).
2) Song S, Tian B, Chen F, Zhang W, Pan Y, Zhang Q, et al. Potentials of proniosomes for improving the oral bioavailability of poorly water-soluble drugs. Drug Dev Ind Pharm. 2015;41(1).
3) Blazek-Welsh AI, Rhodes DG. Maltodextrin-based proniosomes. AAPS PharmSci. 2001 Mar 5;3(1):1–8.
4) Ibrahim MMA, Sammour OA, Hammad MA, Megrab NA. In vitro evaluation of proniosomes as a drug carrier for flurbiprofen. AAPS PharmSciTech. 2008;9(3).
5) Hu C, Rhodes DG. Proniosomes: A novel drug carrier preparation. Int J Pharm. 1999;185(1).
6) Vora B, Khopade AJ, Jain NK. Proniosome based transdermal delivery of levonorgestrel for effective contraception. Journal of Controlled Release. 1998;54(2).
7) Vyas SP, Khar RK. Targeted and controlled drug delivery: novel carrier systems. New Delhi: CBS Publications.
8) Yoshioka T, Sternberg B, Florence AT. Preparation and properties of vesicles (niosomes) of sorbitan monoesters (Span 20, 40, 60 and 80) and a sorbitan triester (Span 85). Int J Pharm. 1994;105(1).
9) Blazek-Welsh AI, Rhodes DG. SEM imaging predicts quality of niosomes from maltodextrin-based proniosomes. Pharm Res. 2001;18(5).
10) 10. Boddu M, Choppari V, Rapalli VK, Badam M. Formulation and Evaluation of Proniosomes of Felodipine. Drug Des. 2017;06(03).